

Exclusive $b\bar{b}$ pair production and irreducible background to the exclusive Higgs boson production

Rafal Maciula¹, Roman Pasechnik², and Antoni Szczurek^{1,3}

¹*Institute of Nuclear Physics PAN, PL-31-342 Cracow, Poland*

²*Uppsala University, Box 516, SE-751 20 Uppsala, Sweden and*

³*University of Rzeszów, PL-35-959 Rzeszów, Poland*

We calculated the cross section for the exclusive double diffractive $b\bar{b}$ production in $pp \rightarrow p(b\bar{b})p$ reaction at LHC. Large cross sections are obtained (3 – 10 nb). This process constitutes the irreducible background to the exclusive Higgs production and is of particular importance in the upcoming Higgs boson searches. The distribution in invariant mass of the $b\bar{b}$ pair is calculated and compared with the corresponding contribution from the Higgs decay. The contribution from the exclusive production of Z^0 and its decay as well as the contribution from the $\gamma\gamma \rightarrow b\bar{b}$ subprocess are also presented for the first time. The influence of cuts on the signal-to-background ratio is discussed.

The identification of the Higgs boson produced in high-energy proton-proton collisions is one of the main goals of the LHC program. The dominant mechanisms of its production are the gluon-gluon and WW fusions. The Higgs boson will be searched for in different decay channels: $b\bar{b}$, $\gamma\gamma$, $\tau^+\tau^-$, W^+W^- , etc., in typical inclusive measurements, i.e. when only the selected decay channel is studied, and the Higgs boson is produced in association with many other particles. Depending on the Higgs mass, the different channels seem more favorable, and each of the decay channels has its own difficulties for the experimental identification.

An alternative solution was suggested already some time ago. It was proposed to identify the Higgs boson in exclusive process $pp \rightarrow pHp$ in the central rapidity region [1–3]. Modern estimates of the corresponding cross section in the k_t -factorization approach with the help of unintegrated gluon distribution functions (UGDFs) have been presented in Ref. [4]. It was argued that in the forward scattering limit the background in the $b\bar{b}$ channel should be small due to the so-called “ $J_z = 0$ selection rule” and a suppression for massless quarks in this channel (see, for example, Ref. [5] and references therein). In general, there is also contribution in the $J_z = 2$ channel and the b -quarks are rather heavy in comparison with the typical soft hadronic scale. Therefore, a realistic estimate of the background requires a real calculation for the genuine four-body reaction $pp \rightarrow p(b\bar{b})p$. The diffractive mechanism of the exclusive $b\bar{b}$ production is shown in Fig. 1. For comparison, we also show the mechanism with intermediate Higgs boson, which is a signal in our analysis and a reaction with the $\gamma\gamma \rightarrow b\bar{b}$ subprocess.

The amplitude for the exclusive process $pp \rightarrow p(q\bar{q})p$

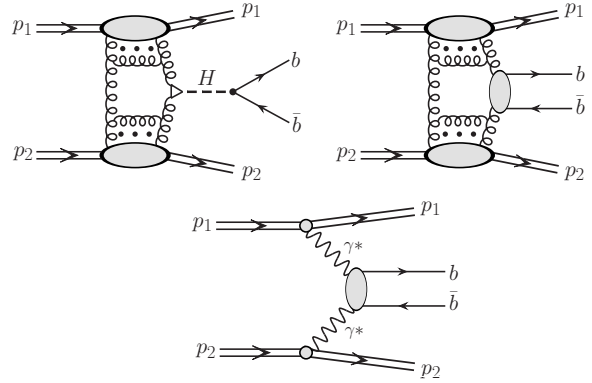


FIG. 1: The diagrams for the $b\bar{b}$ pair production proceeding through the Higgs boson (top-left), the exclusive diffractive $b\bar{b}$ production (top-right) and photon-photon fusion (bottom).

can be written as [4]

$$\mathcal{M}_{\lambda_b \lambda_{\bar{b}}} = \frac{s}{2} \cdot \frac{\pi^2 \delta_{c_1 c_2}}{N_c^2 - 1} \Im \int d^2 q_{0,t} V_{\lambda_b \lambda_{\bar{b}}}^{c_1 c_2}(q_1, q_2, k_1, k_2) \times \frac{f_{g,1}^{\text{off}}(x_1, x'_1, q_{0,t}^2, q_{1,t}^2, t_1) f_{g,2}^{\text{off}}(x_2, x'_2, q_{0,t}^2, q_{2,t}^2, t_2)}{q_{0,t}^2 q_{1,t}^2 q_{2,t}^2}, \quad (1)$$

where $\lambda_q, \lambda_{\bar{q}}$ are helicities of heavy q and \bar{q} , respectively, $t_{1,2}$ are the momentum transfers along each proton line, $q_{1,t}, q_{2,t}, x_{1,2}$ and $q_{0,t}, x'_1 \sim x'_2 \ll x_{1,2}$ are the transverse momenta and the longitudinal momentum fractions for active and screening gluons, respectively. Above $f_{g,1/2}^{\text{off}}$ are the off-diagonal UGDFs of both nucleons. In the calculations presented here we take $\mu^2 = M_{b\bar{b}}^2$, where $M_{b\bar{b}}$ is the invariant mass of the $b\bar{b}$ system. This is consistent with using $\mu^2 = M_H^2 = M_{b\bar{b}}^2$ for exclusive Higgs boson production, which is preferred from the theoretical point of view [7]. The hard $g^*g^* \rightarrow b\bar{b}$ subprocess amplitude $V_{\lambda_q \lambda_{\bar{q}}}$ consists of the Higgs decay signal $g^*g^* \rightarrow H \rightarrow b\bar{b}$ and background contributions, where

the major ones come from the direct $g^*g^* \rightarrow b\bar{b}$ process, from the photon-photon fusion and from the exclusive production of Z^0 and its subsequent decay $Z^0 \rightarrow b\bar{b}$. Note, that due to integration over $\mathbf{q}_{0,t}$ in the diffractive amplitude (1), only symmetric part of the hard subprocess amplitude $V_{\lambda_q\lambda_{\bar{q}}}(\mathbf{q}_{0,t}) = V_{\lambda_q\lambda_{\bar{q}}}(-\mathbf{q}_{0,t})$ contributes to the diffractive cross section.

The off-diagonal UGDFs are written as [8]

$$f_g^{\text{off}}(x', x_{1,2}, q_{1,2t}^2, q_{0,t}^2, \mu_F^2) \simeq R_g f_g(x_{1,2}, q_{1,2t}^2, \mu_F^2), \quad (2)$$

where $R_g \simeq 1.2$ which accounts for the single log Q^2 skewed effect [9]. In the considered kinematics the diagonal unintegrated densities can be written in terms of the conventional (integrated) densities $xg(x, q_t^2)$ as [8]

$$f_g(x, q_t^2, \mu^2) = \frac{\partial}{\partial \ln q_t^2} [xg(x, q_t^2) \sqrt{T_g(q_t^2, \mu^2)}], \quad (3)$$

where T_g is the conventional Sudakov survival factor which suppresses real emissions from the active gluon during the evolution, so the rapidity gaps survive. The gluon q_t 's typical for the central exclusive Higgs production at LHC are of the order of few GeV [4].

Additionally, following to Ref. [7] we use the factorization scale $\mu_F = M_{b\bar{b},t}$ given by the transverse mass of the $b\bar{b}$ pair $M_{b\bar{b},t}$ as compared to the KMR convention [4] $\mu_F^{\text{KMR}} = M_{b\bar{b},t}/2$. We will discuss uncertainties due to sensitivity to the factorization scale μ_F choice and conventional gluon densities $xg(x, q_t^2)$ at small x and q_t below when presenting numerical results.

In the framework of the k_t -factorization approach [10] the hard subprocess $g^*g^* \rightarrow q\bar{q}$ gauge invariant amplitude reads

$$\begin{aligned} V_{\lambda_q\lambda_{\bar{q}}}^{c_1c_2}(q_1, q_2) &\equiv n_\mu^+ n_\nu^- V_{\lambda_q\lambda_{\bar{q}}}^{c_1c_2, \mu\nu}(q_1, q_2), \quad n_\mu^\mp = \frac{p_{1,2}^\mu}{E_{p,cm_s}}, \\ V_{\lambda_q\lambda_{\bar{q}}}^{c_1c_2, \mu\nu}(q_1, q_2) &= -g_s^2 \sum_{i,k} \langle 3i, \bar{3}k | 1 \rangle \bar{u}_{\lambda_q}(k_1) \times \\ &(t_{ij}^{c_1} t_{jk}^{c_2} b^{\mu\nu}(k_1, k_2) - t_{kj}^{c_2} t_{ji}^{c_1} \bar{b}^{\mu\nu}(k_2, k_1)) v_{\lambda_{\bar{q}}}(k_2), \end{aligned} \quad (4)$$

where $E_{p,cm_s} = \sqrt{s}/2$ is the c.m.s. proton energy, t^c are the color group generators in the fundamental representation, $u(k_1)$ and $v(k_2)$ are on-shell quark and antiquark spinors, respectively, b, \bar{b} are the effective vertices arising from the Feynman rules in quasi-multi-Regge kinematics (QMRK) approach illustrated in Fig. 2:

$$\begin{aligned} b^{\mu\nu}(k_1, k_2) &= \gamma^\nu \frac{\hat{q}_1 - \hat{k}_1 - m_q}{(q_1 - k_1)^2 - m^2} \gamma^\mu - \frac{\gamma_\beta \Gamma^{\mu\nu\beta}(q_1, q_2)}{(k_1 + k_2)^2}, \quad (5) \\ \bar{b}^{\mu\nu}(k_2, k_1) &= \gamma^\mu \frac{\hat{q}_1 - \hat{k}_2 + m_q}{(q_1 - k_2)^2 - m^2} \gamma^\nu - \frac{\gamma_\beta \Gamma^{\mu\nu\beta}(q_1, q_2)}{(k_1 + k_2)^2}, \end{aligned}$$

where $\Gamma^{\mu\nu\beta}(q_1, q_2)$ is the effective three-gluon vertex. These effective vertices were initially proposed for massless quarks in Ref. [11] and then extended for massive

case in Ref. [10, 12]. The effective ggg -vertices are canceled out when projecting the $q\bar{q}$ production amplitude Eq. (4) onto the color singlet state, so only the first two diagrams in Fig. 2 contribute to the final result for the production amplitude. Since we will adopt the definition of gluon polarization vectors proportional to transverse momenta $q_{1/2\perp}$, i.e. $\varepsilon_{1,2} \sim q_{1/2\perp}/x_{1,2}$ (see below), then we must take into account the longitudinal momenta in the numerators of effective vertices (see Eq. (5)).

The SU(3) Clebsch-Gordan coefficient $\langle 3i, \bar{3}k | 1 \rangle = \delta^{ik}/\sqrt{N_c}$ in Eq. (4) projects out the color quantum numbers of the $q\bar{q}$ pair onto the color singlet state. Factor $1/\sqrt{N_c}$ provides the averaging of the matrix element squared over intermediate color states of quarks.

Therefore, we have the following amplitude

$$\begin{aligned} V_{\lambda_q\lambda_{\bar{q}}}^{c_1c_2, \mu\nu} &= -\frac{g_s^2}{2} \delta^{c_1c_2} \bar{u}_{\lambda_q}(k_1) \left(\gamma^\nu \frac{\hat{q}_1 - \hat{k}_1 - m}{(q_1 - k_1)^2 - m^2} \gamma^\mu \right. \\ &\left. - \gamma^\mu \frac{\hat{q}_1 - \hat{k}_2 + m}{(q_1 - k_2)^2 - m^2} \gamma^\nu \right) v_{\lambda_{\bar{q}}}(k_2). \end{aligned} \quad (6)$$

Taking into account momentum conservation and using the gauge invariance property, we get the following projection to the light cone vectors (so called ‘‘Gribov’s trick’’)

$$\begin{aligned} V_{\lambda_q\lambda_{\bar{q}}}^{c_1c_2} &= n_\mu^+ n_\nu^- V_{\lambda_q\lambda_{\bar{q}}}^{c_1c_2, \mu\nu} = \frac{4}{s} \frac{q_{1\perp}^\nu - q_{1\perp}^\nu}{x_1} \frac{q_{2\perp}^\mu - q_{2\perp}^\mu}{x_2} V_{\lambda_q\lambda_{\bar{q}}}^{c_1c_2, \mu\nu} \\ &= \frac{4}{s} \frac{q_{1\perp}^\nu}{x_1} \frac{q_{2\perp}^\mu}{x_2} V_{\lambda_q\lambda_{\bar{q}}}^{c_1c_2, \mu\nu}. \end{aligned}$$

Last expression shows that an important consequence of the gauge invariance is the vanishing of the matrix element of the effective $ggq\bar{q}$ -vertex between on-mass-shell quark and antiquark states in the limit of small $q_{1\perp}$ and $q_{2\perp}$ [10, 12]

$$V_{\lambda_q\lambda_{\bar{q}}}^{c_1c_2} \rightarrow 0 \quad \text{for } q_{1\perp} \text{ or } q_{2\perp} \rightarrow 0, \quad (7)$$

The amplitude (6), projected out onto a particular quarkonium state, was successfully applied for the description of the recent CDF data on the exclusive production of charmonia in Ref. [14]. Here we apply the same formalism for separate b and \bar{b} jets production. This is exactly the same formalism as used recently for the exclusive open charm production in Ref. [6].

In the experimentally important case of the forward proton scattering $\mathbf{p}'_{1,2t} \rightarrow 0$ we have $\mathbf{q}_{1,t} \simeq -\mathbf{q}_{2,t} \simeq \mathbf{q}_{0,t} \equiv \mathbf{q}_t$, and the transverse mass of the $b\bar{b}$ pair in terms of b -quark rapidities $y_{b,\bar{b}}$ reads

$$M_{b\bar{b},t}^2 = M_{b\bar{b}}^2 = 2m_{b,t}^2 (1 + \cosh(y_b - y_{\bar{b}})) \quad (8)$$

If one looks at centrally produced b -jets only, i.e. $y_{b,\bar{b}} \rightarrow 0$, then according to Eq. (8) the only way to produce the large invariant mass $M_{b\bar{b}} \sim M_H$ is to consider high- k_t jets limit $k_t \gg m_b, q_t$. The amplitude V_{+-} vanishes for jets

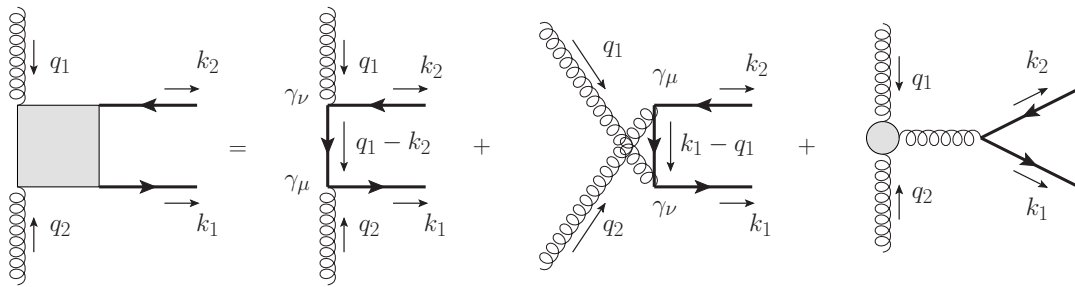


FIG. 2: Effective vertex in the QMRK approach [11]. Last diagram with effective 3-gluon vertex drops out in projection to the color singlet final state.

with very small rapidities, i.e. when $y_b \sim y_{\bar{b}} \rightarrow 0$. Amplitude V_{++} behaves as $\sim q_t^2 \cos \phi / k_t^2$ and thus extremely suppressed in the high- k_t limit. This is in agreement with the statement that Higgs CEP background is suppressed in very forward and quark massless limits for centrally produced $b\bar{b}$ jets (with small rapidities), and agrees with the $J_z = 0$ selection rule [15].

However, the particular high- k_t limit is only a part of the whole story. In our previous analysis of the exclusive open charm production in Ref. [6] it was shown that the dominant contribution to the $c\bar{c}$ dijet cross section comes from relatively small quark transverse momenta $k_t \simeq 1$ GeV. The same should hold for exclusive $b\bar{b}$ pair production relevant for the Higgs background. Indeed, resolving relation (8) with respect to typical rapidity difference $|y_b - y_{\bar{b}}| = \Delta y$ neglecting quark transverse momenta k_t and keeping only the b -mass contributions $m_b \simeq 4.5$ GeV at fixed $M_{b\bar{b}} = 120$ GeV, we get $\Delta y \simeq 6.6$. So, the irreducible background for Higgs CEP can be dominated by b -quarks with comparably small transverse momenta $k_t \ll m_b$, but with rather large rapidities $y_b \sim -y_{\bar{b}} \simeq 3.3$.

In the last kinematical situation the amplitudes $V_{\lambda_b \lambda_{\bar{b}}}$ are not suppressed by a large denominators, and significant contributions can be obtained. For simplicity, keeping only the quark mass $m_b \gg k_t$ and large rapidity $y_b \sim -y_{\bar{b}} \sim 3$ contributions, we get for helicity amplitudes

$$\begin{aligned} V_{++} &\simeq \frac{ig_s^2 |\rho|}{m_b^3 \sqrt{\cosh(y_b) \cosh(y_{\bar{b}})}} \left[|\rho| \kappa - 2\rho |\kappa| \cos \phi \right], \\ V_{+-} &\simeq \frac{-g_s^2 |\rho|^2 \tanh(y_b - y_{\bar{b}})}{m_b^2 \sqrt{\cosh(y_b) \cosh(y_{\bar{b}})}} \end{aligned} \quad (9)$$

where we have introduced the shorthand complex notations in the forward limit

$$\kappa = k^y + ik^x, \quad \rho = q^y + iq^x,$$

for the quark and gluon transverse momenta, respectively.

In this low- k_t regime V_{+-} helicity amplitude is dominated over V_{++} as opposite to the high- k_t case. From Eq. (9) we see that the amplitude is proportional to

$q_t^2 = -|\rho|^2$, which typically can be of the order of few GeV at LHC energy. This means that numerically low- k_t contribution (of course, at not extremely large $y_{b,\bar{b}}$) in the case of b -jets can lead to a dominant contribution to the exclusive background for Higgs CEP. In this asymptotics, the quark mass m_b plays an important role since it comes into the denominator in Eq. (9). Precise evaluation of the corresponding signal, however, demands employing the formulae for the hard amplitudes in the general form in Eq. (6). More detailed analytical and numerical investigation of contributions from different parts of the phase space will be presented elsewhere [16].

In parallel to the total cross section, we calculate the differential cross sections for exclusive Higgs boson production. Compared to the standard KMR approach here we calculate the amplitude with the hard subprocess $g^* g^* \rightarrow H$ taking into account off-shellness of the active gluons, i.e. fully consistent with the exclusive production of the $b\bar{b}$ pairs, where the gluon transverse momenta play crucial role. The details of the off-shell matrix element can be found in Ref. [17]. In contrast to the exclusive χ_c production [14], due to a large factorization scale $\sim M_H$ the off-shell effects for $g^* g^* \rightarrow H$ give only a few percents to the final result.

The same unintegrated gluon distributions based on the collinear distributions are used for the Higgs and continuum $b\bar{b}$ production. This is absolutely necessary for proper estimate of the signal-to-background ratio, the main purpose of the present Letter. In the case of exclusive Higgs production we calculate the four-dimensional distribution in the standard kinematical variables: y, t_1, t_2 and ϕ . Assuming for this presentation the full coverage for outgoing protons¹ we construct the two-dimensional distributions $d\sigma/dy d^2 p_t$ in Higgs rapidity and transverse momentum. The distribution is used then in a simple Monte Carlo code which includes the Higgs boson decay into the $b\bar{b}$ channel. It is checked sub-

¹ The exact comparison with experimental set up requires inclusion of extra cuts on fractional momentum loss of protons and is slightly different for ATLAS and CMS.

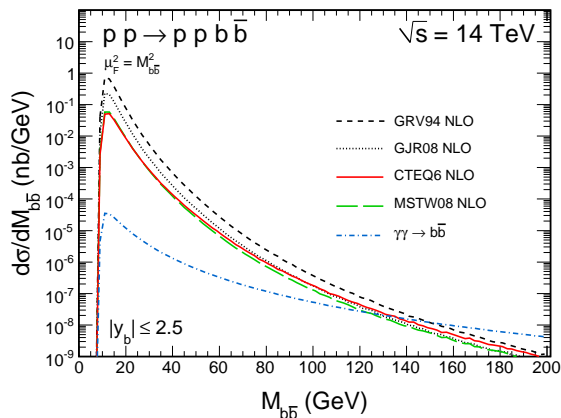


FIG. 3: The $b\bar{b}$ invariant mass distribution for $\sqrt{s} = 14$ TeV and for $-2.5 < y < 2.5$ corresponding to the ATLAS/CMS detectors. The absorption effects were taken into account by multiplying by the gap survival factor $S_G = 0.03$.

sequently whether the b and \bar{b} enter into the pseudorapidity region spanned by the central detector. Including the simple cuts we construct several differential distributions in different kinematical variables.

In general, employing the diagonal UGDF in the form (3) one encounters a problem of poorly known gluon PDFs at rather low $x_{1,2}$ and especially small gluon virtualities q_{\perp}^2 . For an illustration of the corresponding uncertainties, in Fig. 4 we show several parameterizations for the gluon PDFs widely used in the literature as functions of momentum fraction x at the evolution scale $\sim q_{\perp}^2$ fixed at characteristic value 2 GeV^2 typical for the exclusive production of Higgs boson (for quarkonia production it is even smaller leading to huge uncertainties as discussed e.g. in Ref. [14]). We see that at $x \lesssim 10^{-3}$ the PDF uncertainties may strongly affect predictions for not sufficiently large gluon transverse momenta. In this sense, precise data on the diffractive and central exclusive production can be used to constrain the PDF parameterizations [13, 14].

Testing other models of UGDFs different from Eq. (3) may be important for estimation of an overall theoretical uncertainty of our predictions and their stability, and it is planned for our future study.

In the following we shall present the main results. A more detailed analysis with the presentation of several differential distributions will be given elsewhere [16]. In Fig. 3 we show the most essential distribution in the invariant mass of the centrally produced $b\bar{b}$ pair, which is also being the missing mass of the two outgoing protons. In this calculation we have taken into account typical detector limitations in rapidity $-2.5 < y_b, y_{\bar{b}} < 2.5$. We show results with different collinear gluon distributions from the literature: GRV [18], CTEQ [19], GJR [21] and MSTW [20]. The results obtained with radiatively gen-

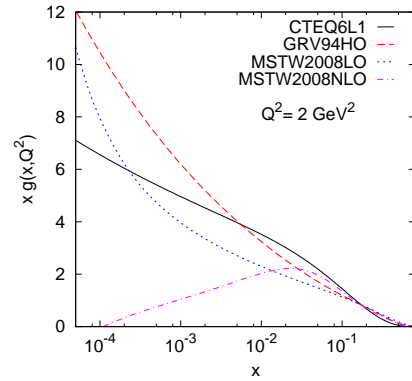


FIG. 4: Illustration of the gluon densities as functions of the longitudinal momentum fraction x at the characteristic factorisation scale $Q^2 = 2 \text{ GeV}^2$ (typical for the central exclusive production processes) given by the global parameterizations CTEQ6L1 [19], GRV94HO [18], MSTW2008LO and NLO [20].

erated gluon distributions (GRV, GJR) allow to use low values of $Q_t = q_{0,t}, q_{1,t}, q_{2,t}$ whereas for other gluon distributions an upper cut on Q_t is necessary. The integrated double-diffractive $b\bar{b}$ contribution calculated here seems bigger than the contribution of the exclusive photoproduction of $b\bar{b}$ estimated in [22] and details require systematic studies in the future. The lowest curve in Fig. 3 represents the $\gamma\gamma$ contribution (the bottom diagram in Fig. 1). While the integrated over phase space $\gamma\gamma$ contribution is rather small, is significant compared to the double-diffractive component at large $M_{b\bar{b}} > 100 \text{ GeV}$. This can be understood by damping of the double diffractive component at large $M_{b\bar{b}}$ by the Sudakov form factor [4, 6]. In addition, in contrast to the double-diffractive component the absorption for the $\gamma\gamma$ component is very small and in practice can be neglected.

In the top panel of Fig. 5 we show the double diffractive contribution for a selected (CTEQ6 [19]) collinear gluon distribution and the contribution from the decay of the Higgs boson including natural decay width calculated as in Ref. [23], see the sharp peak at $M_{b\bar{b}} = 120 \text{ GeV}$ (assumed arbitrarily for illustration), which is not excluded at present by the Higgs searches at LEP [24] and Tevatron [25]. The phase space integrated cross section for the Higgs production, including absorption effects with $S_G = 0.03$ is slightly less than 1 fb which is similar to that predicted by the KMR group. This value is similar as in many KMR evaluations [4]. The result shown in Fig. 5 includes also the branching fraction for $\text{BR}(H \rightarrow b\bar{b}) \approx 0.8$ and the rapidity restrictions. The second much broader Breit-Wigner type peak corresponds to the exclusive production of the Z^0 boson with the cross section calculated as in Ref. [26]. The exclusive cross section for $\sqrt{s} = 14 \text{ TeV}$ is 16.61 fb including absorption (28.71 fb without absorption effects). The branching fraction $\text{BR}(Z^0 \rightarrow b\bar{b}) \approx$

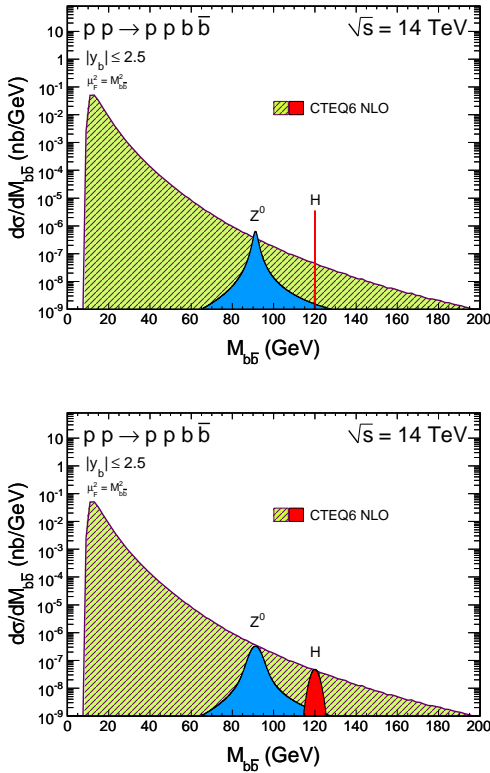


FIG. 5: The $b\bar{b}$ invariant mass distribution for $\sqrt{s} = 14$ TeV and for b and \bar{b} jets in the rapidity interval $-2.5 < y < 2.5$ corresponding to the ATLAS detector. The absorption effects for the Higgs boson and the background were taken into account by multiplying by the gap survival factor $S_G = 0.03$. The top panel shows purely theoretical predictions, while the bottom panel includes experimental effects due to experimental uncertainty in invariant mass measurement.

0.15 has been included in addition. In contrast to the Higgs case the absorption effects for the Z^0 production are much smaller [26]. The sharp peak corresponding to the Higgs boson clearly sticks above the background. In the above calculations we have assumed an ideal no-error measurement.

In reality the situation is, however, much worse as both protons and in particular b and \bar{b} jets are measured with a certain precision which automatically leads to a smearing in $M_{b\bar{b}}$. While such a smearing is negligible for the background, it leads to a significant modification of the Breit-Wigner peaks, especially of the sharp one for the Higgs boson. In the present Letter the experimental effects are included in the simplest way by a convolution of the theoretical distributions with the Gaussian smearing function

$$G(M) = \frac{1}{\sqrt{2\pi}\sigma} \exp\left(-\frac{(M - M_H)^2}{2\sigma^2}\right), \quad (10)$$

with $\sigma = 2$ GeV, which realistically represents the experimental situation [27, 28] and is determined mainly

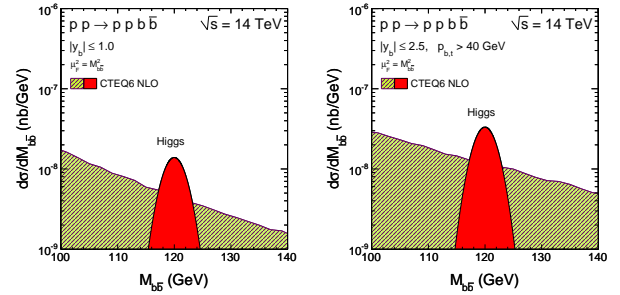


FIG. 6: The $b\bar{b}$ invariant mass distribution for $\sqrt{s} = 14$ TeV for a limited range of b and \bar{b} rapidities: $-1 < y < 1$ (left) and for $p_{t,2t} < 0.4$ GeV (right).

by the precision of measuring forward protons. In the bottom panel we show the invariant mass distribution when the invariant mass smearing is included. Now the bump corresponding to the Higgs boson is below the $b\bar{b}$ background. With the experimental resolution assumed above the identification of the Standard Model Higgs will be rather difficult. The situation for some scenarios beyond the Standard Model may be better [16].

The question now is whether the situation can be improved by imposing further cuts. In Fig. 6 (left panel) we show the result for a more limited range of b and \bar{b} rapidity, i.e. not making use of the whole coverage of the main LHC detectors. Here we omit the Z^0 contribution and concentrate solely on the Higgs signal. Now the signal-to-background ratio is somewhat improved. This would be obviously at the expense of a deteriorated statistics. Similar improvements of the signal-to-background ratio can be obtained by limiting transverse momenta of outgoing protons (right panel).

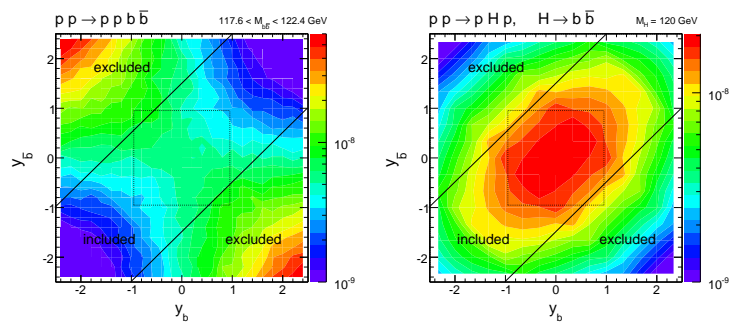


FIG. 7: Two-dimensional distributions over b and \bar{b} rapidities for QCD background (left panel), and Higgs CEP signal (right panel) with the optimal two-dimensional cut in the $(y_b, y_{\bar{b}})$ space is marked by the thick contours.

In order to preserve statistics and to remove most of the $b\bar{b}$ background we have to impose more specific two-dimensional cuts. An example is shown in Fig. 7. Indeed, considering only the band between two thick solid lines

would remove most of the $b\bar{b}$ background, concentrated mainly in regions with relatively large difference between quark and antiquark rapidities $|y_b - y_{\bar{b}}| \gtrsim 1$ (see, the left panel in Fig. 7). At the same time, such a cut allows to keep most of the Higgs signal, which is concentrated in the central rapidity region $y_{b,\bar{b}} \approx 0$, as oppose to the background (see, the right panel in Fig. 7).

In the present analysis we have not been interested in the precise estimation of the cross section but rather in understanding the signal-to-background ratio which is of the major importance for the upcoming Higgs boson searches at the LHC. Consequently, we have presented results with only one UGDF. This ratio is practically the same for other UGDFs, which will be shown explicitly in [16]. The absorption effects have been included here in a simple multiplicative form. They are expected to be the same both for the signal and the background, and thus are not affecting the ratio under consideration. The same gap survival factor has been used in both cases.

The overall theoretical uncertainty of our predictions for the absolute value of the $b\bar{b}$ background contribution is estimated to be the same as for the Higgs CEP, and given by a factor of 3 more/less [4]. Theoretical uncertainty in the signal-to-background ratio under consideration is typically much smaller, as the main part of the uncertainty coming from the normalisation of UGDFs (R_g factor) and absorbtive effects (gap survival S_G factor) is common for both contributions and thus canceled out in the ratio.

In our analysis we have been concentrated on the irreducible background only. Other contributions, although, in principle, reducible, can in practice be also rather troublesome [29]. These include dijet misidentification (mainly due to the $gg \rightarrow gg$ subprocess), inclusive double-pomeron processes [30] and multi-event effects related to large luminosity [29]. Further analyses, especially for the Standard Model Higgs boson production, seem to be necessary to understand whether the Higgs boson can be identified in the exclusive production, perhaps not only in the $b\bar{b}$ decay channel. The present parton level analysis should be supplemented in the future by additional analysis of $b\bar{b}$ jets by including a model of hadronization. Then standard jet algorithms could be imposed and the quality of the b and \bar{b} kinematical reconstruction could be studied in detail.

We are indebted to Valery Khoze, Oleg Teryaev for a discussion of central diffraction, to Andy Pilkington and Christophe Royon for a discussion of experimental limitations of the exclusive processes discussed in this letter and Ania Cisek for providing us numerical results of the exclusive Z^0 production from Ref. [26]. This work was partially supported by the Polish grant of MNiSW N N202 249235 and by the Carl Trygger Foundation.

-
- [1] A. Schäfer, O. Nachtmann and R. Schöpf, Phys. Lett. **B249** (1990) 331.
 - [2] A. Białas and P.V. Landshoff, Phys. Lett. **B256** (1991) 540.
 - [3] J.-R. Cudell and O.F. Hernandez, Nucl. Phys. **B471** (1996) 471.
 - [4] V. A. Khoze, A. D. Martin and M. G. Ryskin, Phys. Lett. B **401**, 330 (1997);
A. B. Kaidalov, V. A. Khoze, A. D. Martin and M. G. Ryskin, Eur. Phys. J. C **33**, 261 (2004).
 - [5] V. A. Khoze, M. G. Ryskin and A. D. Martin, Eur. Phys. J. C **64**, 361 (2009).
 - [6] R. Maciula, R. Pasechnik and A. Szczurek, Phys. Lett. B **685**, 165 (2010).
 - [7] T. D. Coughlin and J. R. Forshaw, JHEP **1001**, 121 (2010).
 - [8] M. A. Kimber, A. D. Martin and M. G. Ryskin, Phys. Rev. D **63**, 114027 (2001);
A. D. Martin and M. G. Ryskin, Phys. Rev. D **64**, 094017 (2001).
 - [9] A. G. Shuvaev, K. J. Golec-Biernat, A. D. Martin and M. G. Ryskin, Phys. Rev. D **60**, 014015 (1999).
 - [10] P. Hagler, R. Kirschner, A. Schafer, L. Szymanowski and O. Teryaev, Phys. Rev. D **62**, 071502 (2000);
P. Hagler, R. Kirschner, A. Schafer, L. Szymanowski and O. V. Teryaev, Phys. Rev. Lett. **86**, 1446 (2001).
 - [11] V. S. Fadin and L. N. Lipatov, Nucl. Phys. B **477**, 767 (1996) [arXiv:hep-ph/9602287].
 - [12] P. Hagler, R. Kirschner, A. Schafer, L. Szymanowski and O. Teryaev, Phys. Rev. D **62**, 071502 (2000) [arXiv:hep-ph/0002077].
 - [13] R. Pasechnik, R. Enberg and G. Ingelman, Phys. Rev. D **82**, 054036 (2010) [arXiv:1005.3399 [hep-ph]];
R. Pasechnik, R. Enberg and G. Ingelman, arXiv:1004.2912 [hep-ph].
 - [14] R. S. Pasechnik, A. Szczurek and O. V. Teryaev, Phys. Rev. D **78**, 014007 (2008);
R. S. Pasechnik, A. Szczurek and O. V. Teryaev, Phys. Lett. B **680**, 62 (2009);
R. S. Pasechnik, A. Szczurek and O. V. Teryaev, Phys. Rev. D **81**, 034024 (2010).
 - [15] V. A. Khoze, A. D. Martin and M. G. Ryskin, Eur. Phys. J. C **19**, 477 (2001) [Erratum-ibid. C **20**, 599 (2001)].
 - [16] R. Maciula, R.S. Pasechnik and A. Szczurek, a work in preparation.
 - [17] R. S. Pasechnik, O. V. Teryaev and A. Szczurek, Eur. Phys. J. C **47**, 429 (2006).
 - [18] M. Glück, E. Reya and A. Vogt, Z. Phys. **C67**, 433 (1995).
 - [19] J. Pumplin et al., JHEP **0207**, 012 (2002).
 - [20] A.D. Martin et al., Eur. Phys. J. **C63**, 189 (2009).
 - [21] M. Glück, D. Jimenez-Delgado, E. Reya, Eur. Phys. J. **C53**, 355 (2008).
 - [22] V.P. Goncalves and M.V.T. Machado, Phys. Rev. **D75**, 031502(R) (2007).
 - [23] G. Passarino, Nucl. Phys. B **488**, 3 (1997).
 - [24] ALEPH, DELPHI, L3, OPAL, and SLD Collaborations, LEP Electroweak Working Group, SLD Electroweak Group, SLD Heavy Flavour Group, Phys. Rept. **427**, 257 (2006);
ALEPH, CDF, D0, DELPHI, L3, OPAL, and SLD Col-

- laborations, LEP Electroweak Working Group, Tevatron Electroweak Working Group, SLD electroweak heavy flavour groups, arXiv:0911.2604.
- [25] A. Dominguez, AIP Conf. Proc. **1182**, 138 (2009); CDF and D0 Collaborations, Tevatron New Physics and Higgs Working Group, arXiv:0911.3930.
- [26] A. Cisek, W. Schäfer and A. Szczurek, Phys. Rev. **D80** 074013 (2009).
- [27] A. Pilkington, private communication.
- [28] Ch. Royon, private communication.
- [29] B.E. Cox, F.K. Loebinger and A.D. Pilkington, JHEP 0710, 090 (2007).
- [30] M. Boonekamp, R. Peschanski and C. Royon, Phys. Rev. Lett. **87** 251806 (2001).

$p p \rightarrow p p b \bar{b}$

$M_{b\bar{b}} \in (110, 130) \text{ GeV}$

